NONLINEAR DEFLECTIONS OF A PIN ENDED SLENDER BEAM COLUMN OF ARBITRARY STIFFNESS

by

Michael Duane Calderwood

B.S., Kansas State University, 1974

A MASTER'S THESIS

submitted in partial fulfillment of the

requirements for the degree

MASTER OF SCIENCE

Department of Mechanical Engineering

KANSAS STATE UNIVERSITY
Manhattan, Kansas

1977

Approved:

Major Professor

TABLE OF CONTENTS

LIST OF FIGURES

LIST OF TABLES

NOMENCLATURE

EI,β	pole stiffness ($lb \cdot in^2$)
F	side load
F_x	x component of side load
F_y	y component of side load
ℓ	length between supports in experimental stiffness determination
L	length of beam column
M	bending moment
M_F	bending moment due to the side load
M_w	bending moment due to the distributed load
M1,M2,M3,Y1,Y2,Y3	dummy dependent variables
N	force used in experimental stiffness determination
P	buckling force - lies on x axis
R_1	reaction force at s=L
R_2	reaction force at s=0
R	total reaction force $R=R_1+R_2$
R1,R2,θ1,θ2	dummy independent variables
s,θ	axial curvilinear coordinate system
$\bar{s},\bar{x}$	dummy integration variables
s_F, x_F, y_F	coordinate of the side load
V	experimental voltage reading
V_{tare}	experimental voltage reading at no load
w	distributed load (lbs/in.)
x,y	rectangular coordinate system
δ	maximum y deflection

NOMENCLATURE (Continued)

$\delta\theta, \delta R$	perturbations of θ or R
Δ	deflection in experimental stiffness determination
ϕ	angular direction of side load
dx/ds	derivative of x with respect to s
$\partial x/\partial s$	partial derivative of x with respect to s

INTRODUCTION

The first published analysis concerned with buckling of the elastica was made by Leonhard Euler in the 1700's (9). In this paper, Euler recognized the existence of a critical buckling load and states: "Therefore, unless the load P to be borne be greater than $c\pi^2/4\ell^2$, there will be absolutely no fear of bending; on the other hand, if the weight P be greater, the column will be unable to resist bending." Since then, the shape of this uniform column under the load P has been determined using eliptic integrals (2,10) or by direct integration of an infinite series (4).

Although this information has been known for many years, the literature has a notable lack of information concerning large elastic deflections of either nonuniform columns or nonuniform beam columns. The emphasis in recent years has generally been on uniform beams and beam columns (7), and often then primarily concerned with the critical loadings (1). This is understandable as structural members are usually designed to eliminate both failure and large deflections. This, and the limited elastic range of many structural materials precludes concern with large deflection analysis of most structural members.

However, there is a demand for knowledge of large deflection buckling due to the use of the elastica as a spring. A spring of this type has the advantage of limiting deflections to a specific loading range, while common springs not only deflect over this range but also deflect from zero load up to the desired range. A specific example of this use is the pole vaulting pole. The pole is to be nearly straight with just the weight of the vaulter, yet undergo large deflections due to an impact loading at the beginning of the vault. Any model of this beam column must accurately predict deflections for a prescribed loading in the large deflection range.

Recently, Walker and Kirmser (11) determined numerically the post buckling behavior of a pin ended slender column of arbitrary stiffness distribution using the shooting method. This technique proved to be convenient, inexpensive, and easy to use for the problem considered.

This thesis uses the technique presented by Walker and Kirmser to determine the load deflection relationships for a pin ended slender beam column of arbitrary stiffness distribution. The stiffness must be continuous along the elastica and is assumed to obey Hooke's law. Loading is restricted to a point load, a uniformly distributed load, and a buckling load. Also presented is a physical model of the elastica. Experimental data were collected and comparisons made between the physical and numerical solutions.

THIS BOOK CONTAINS NUMEROUS PAGES WITH DIAGRAMS THAT ARE CROOKED COMPARED TO THE REST OF THE INFORMATION ON THE PAGE.

THIS IS AS RECEIVED FROM CUSTOMER.

DERIVATION OF EQUATIONS

The pin ended elastica was modeled as the slender beam column of arbitrary stiffness distribution shown in Figure 1. The stiffness distribution is continuous and the elastic properties were assumed to obey Hooke's law. Consequently, the nonlinearity is purely geometrical.

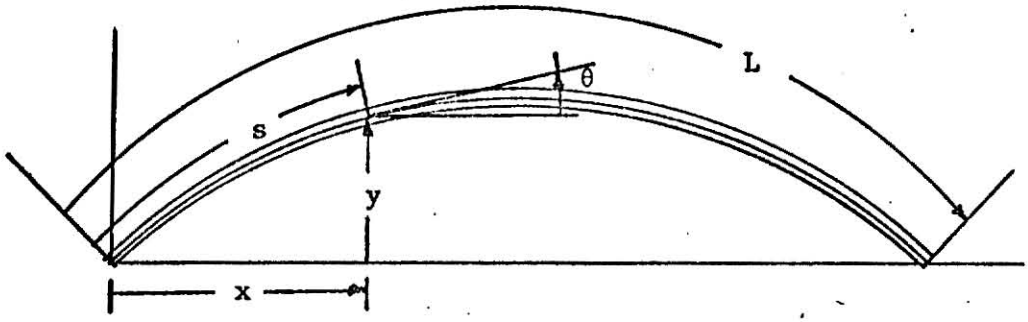

Figure 1

The loadings are shown in Figure 2 and may consist of a buckling force P, a distributed load w which is perpendicular to the longitudinal axis of the unbent pole, and a point load F of arbitrary location, direction, and magnitude.

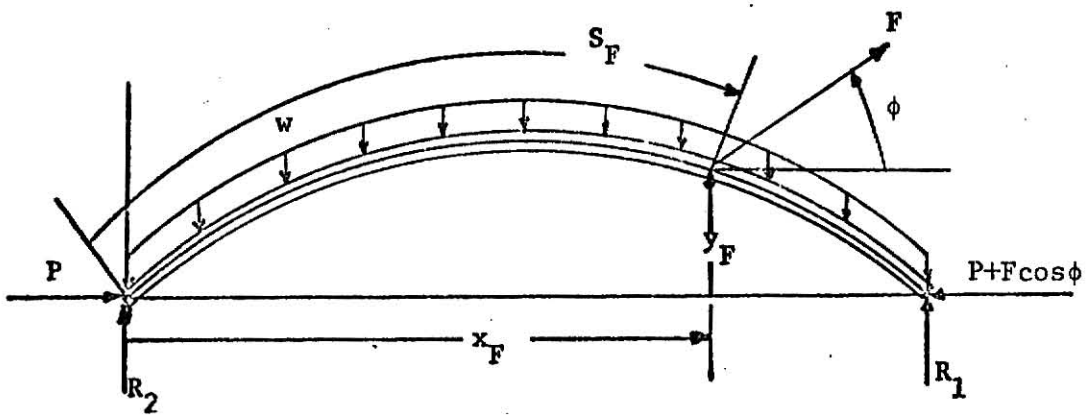

Figure 2

The differential equations and the boundary conditions describing this nonlinear pin ended elastica are:

$$EI \frac{d\theta}{ds} = M \quad (8) \tag{1}$$

$$\frac{dy}{ds} = \sin\theta \tag{2}$$

$$\frac{dx}{ds} = \cos\theta \tag{3}$$

$$y(0) = y(L) = M(0) = M(L) = 0 \tag{4}$$

Consider the section of the beam shown in Figure 3 where $0 \leq s \bar{<} s_F$

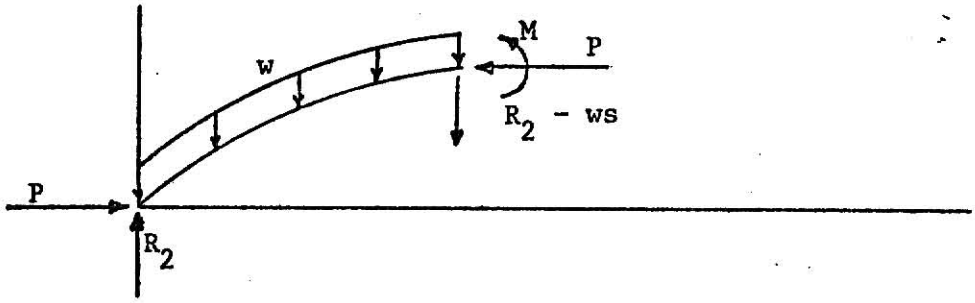

Figure 3

Using the rules of statics, the internal forces at the section were determined, and since

$$\Sigma \bar{M}_{s=0} = 0 = Py + M - (R_2 - ws)x - \int_0^s w\bar{x}d\bar{s}$$

or

$$M = -Py + (R_2 - ws)x + \int_0^s w\bar{x}d\bar{s}$$

therefore (1) becomes

$$\frac{d\theta}{ds} = [-Py + (R_2 - ws)x + \int_0^s w\bar{x}d\bar{s}]/EI]$$

Simularily, for the section of the beam shown in Figure 4 where $s_F < s \leq L$

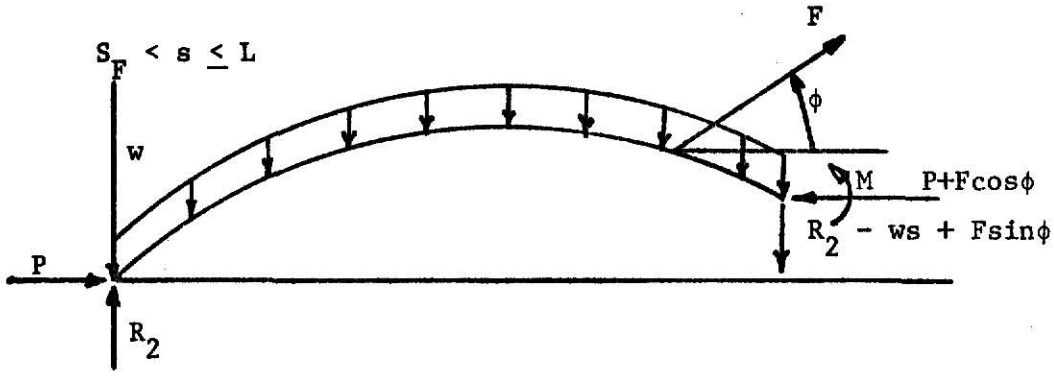

Figure 4

$$\Sigma M_{s=0} = 0 = (P + F\cos\phi)y + M - (R_2 - ws + F\sin\phi)x - \int_0^s w\bar{x}d\bar{s}$$

$$- F\cos\phi y_F + F\sin\phi x_F$$

$$M = -(P + F\cos\phi)y + (R_2 - ws - F\sin\phi)x + \int_0^s w\bar{x}d\bar{s} + F\cos\phi y_F - F\sin\phi x_F$$

therefore (1) becomes

$$\frac{d\theta}{ds} = [-(P + F\cos\phi)y + (R_2 - ws + F\sin\phi)x + \int_0^s w\bar{s}d\bar{s} + F\cos\phi y_F - F\sin\phi x_F]/EI$$

(6)

METHOD OF SOLUTION

The four simultaneous first order differential equations were solved by numerical integration and the shooting method (3,11). The problem was posed as an initial value problem for the given forces P,F, and w by assuming values for the reaction force R_2 and the initial slope of the beam column $\theta(0)$.

In order to determine the magnitude of the moment in the section beyond the side load it was necessary to locate the x and y coordinates of the side load. A technique called Lagrangian interpolation (5) was used to extrapolate these coordinates from the four grid points preceeding the side load. This procedure essentially predicts x_F and y_F from third degree polynomials in the independent variable s.

As it was desirable to supply the elastic constants at discrete, evenly distributed points along the length of the elastica, a single step explicit numerical integration technique was an excellent choice. The fourth order Runge-Kutta-Gill technique (6) with constant step size was selected. Since this technique evaluates the derivatives at the half step points, it was modified to use an average of adjacent stiffness values for those calculations.

Integrating from s=0 to s=L as indicated above provides a solution that satisfies the differential equations and boundary conditions at the s=0 end. By adjusting the assumed values for R_2 and $\theta(0)$ one can generate a solution that satisfies the boundary conditions at both ends. This adjustment was made by considering y(L) and M(L) as functions of $\theta(0)$ and R_2. Using the Taylor series expansion of these functions of two variables, a technique was derived to select the next iterates and is shown in

Appendix A (3). For the case of no side loads, y(L) was considered to be a function of $\theta(0)$ only. This simplification reduces the number of evaluations necessary for selecting the next iterate. This technique is also shown in Appendix A. Note that these techniques are equivalent to modified Newton's methods.

In order to incorporate these procedures into a computer program it was necessary to cast the problem into vector notation. The vector representation is shown in Appendix B. For clarity, the symbols currently used will be retained in this text.

The general approach of the computer program was to select initial values for $\theta(0)$ and R_2. Integrating along the length of the elastica using the Runge-Kutta-Gill technique and Lagrangian extrapolation yields values of y(L) and M(L). By perturbing separately $\theta(0)$ and R_2, three sets of values for y(L) and M(L) were generated. Using these values and the modified Newton's method the values of $\theta(0)$ and R_2 for the next iterate were determined. Repeated application of this process until y(L) and M(L) are zero or within specified accuracies yields the desired solution.

A list of the computer program is shown in Appendix C.

EXPERIMENTAL DETERMINATION OF THE STIFFNESS FUNCTION

The fundamental physical properties that describe the elastica are length and stiffness. The stiffness is the product of Young's modulus E and the moment of inertia of the cross-section I.

A commercial fiberglas pole vaulting pole was selected to simulate the elastica. The cross-section of this pole is annular in shape, with a varying diameter and thickness. The stiffness was dependent upon which cross sectional axis the bending occurred about. Due to these irregularities it was necessary to determine the stiffness experimentally about the weakest axis.

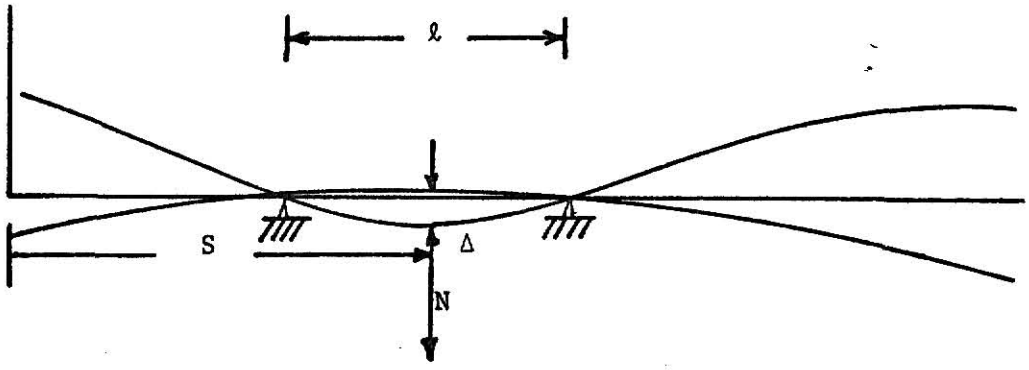

Figure 5.

The procedure used in determining the stiffness function of the pole was based on the linear bending of a simply supported beam and the principle of superposition. The pole was placed over the supports which were separated by a distance ℓ as shown in Figure 5. A load N was applied centrally between the supports and the change in deflection Δ at the loading point due to this load was recorded. The average stiffness for that section of the pole was calculated from the relation

$$EI = \frac{N\ell^3}{48\Delta} \quad .$$

Ideally, ℓ would be selected very small and the average stiffness calculated would represent the stiffness at the point of interest. There are two problems which are encountered with this approach. First, the magnitude of Δ is restricted by the accuracy of the measuring instruments. Measuring Δ with a dial gauge required the magnitude to be several hundredths of an inch. Consequently, as can be seen from equation (7), decreasing ℓ requires a cubic increase in N. The second problem is encountered with large values of N. When the load was applied the annular shape of the pole cross section flattened. This flattening caused misleading values of Δ and the pole appeared to be softer than actually is the case. Due to the importance of these problems it was necessary to use a large ℓ, and the values determined for the stiffness are an average over a four foot length. The stiffness was calculated every foot between two feet and thirteen feet from the pole box end. This data is shown in Table 1 and a plot of the data with a smooth curve drawn through the experimental points is shown in Figure 6.

The extrapolated parts of Figure 6 are shown to level off instead of continuing to decrease. This characteristic is predicted from the method of construction of this pole. The pole was constructed by rolling sheets of fiberglas of varying widths. The number, shape, and location of these sheets determine the stiffness characteristics. It is believed that the stiffness of the ends are reasonably uniform.

Table 1

Standard Pole III

Dura-fiber
Cata-Pole 550+
model 1580+ Flex no 6.125

L = 15' 7"
N = 15.88 lbs
ℓ = 4'

S (ft)	Δ (in.)	EI (psi)	S (ft)	Δ (in.)	EI ($lb \cdot in^2$)
2	.0745	492,000	8	.0545	671,000
3	.0635	576,000	9	.0570	642,000
4	.0554	660,000	10	.0605	605,000
5	.0545	571,000	11	.0695	526,000
6	.0550	665,000	12	.0845	433,000
7	.0545	671,000	13	.1020	359,000

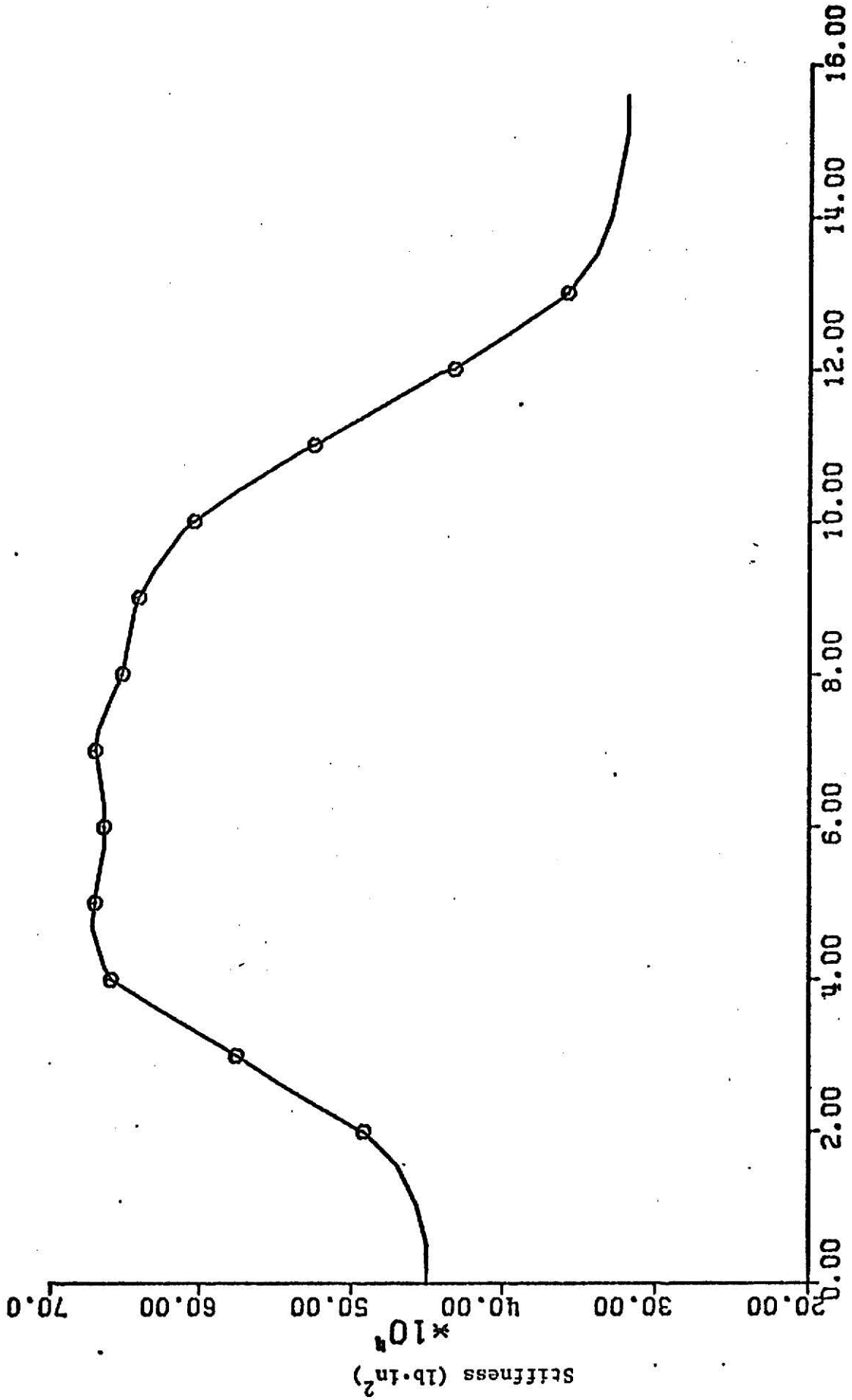

Figure 6. Stiffness function.

EXPERIMENTAL LARGE DEFLECTION BUCKLING

For the purpose of comparison, experimental configurations of the elastica were determined. The apparatus used to obtain these experimental data is shown in Figures 7 and 8. End A has a fixed support on which a statham 200 lb capacity load cell was mounted. The load cell was connected to a 6 volt D.C. battery and a digital voltmeter. The opposite end has a movable support on which a hydraulic cylinder was mounted. These supports were mounted on a channel iron beam which served as a base and reference of orientation. The movable support could be drawn toward end A by the use of a block and tackle and clamped in place after positioning. A single ball bearing at each end provided the hinged end conditions. The bearings were placed between the supports and end caps which were fitted on the pole. Although the problem of friction was not eliminated the lever arm through which the frictional force acted was small. This should provide an adequate approximation of the pinned end conditions.

The pole was placed between the supports with the pole box end at end A. Therefore the force indicated by the load cell was the buckling force P as defined previously.

The pole was buckled, clamped in place, and rotated to determine the weak axis, which represents the axis about which the stiffness was measured. The distributed load was due to the weight of the pole and considered present if the pole was buckled in a horizontal plane and absent if the pole was buckled in a vertical plane. Point loads were applied by either hanging weights (Figure 9) or by the use of spring scales (Figure 10). Once the loading was completed the configuration of the pole was measured or recorded by photograph. P was determined from the voltage output of the transducer by the relation

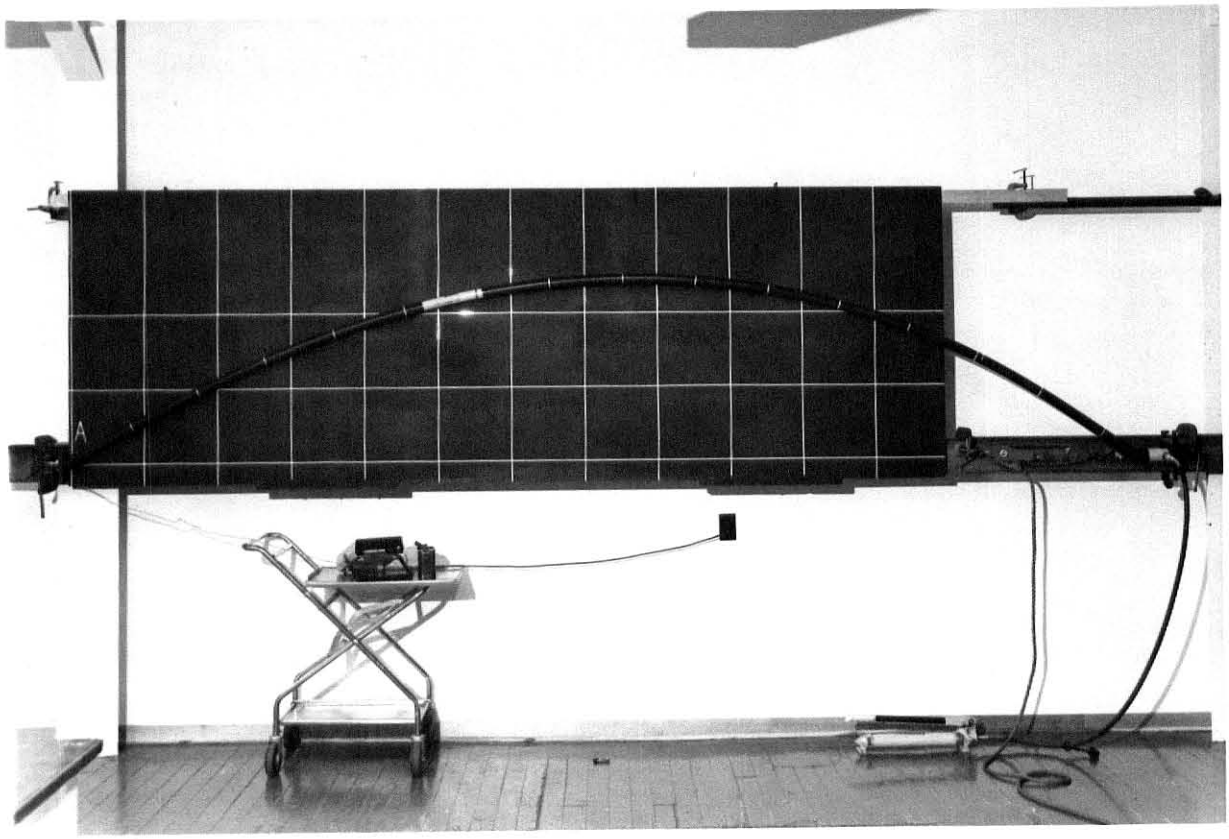

Figure 7. Experimental Apparatus

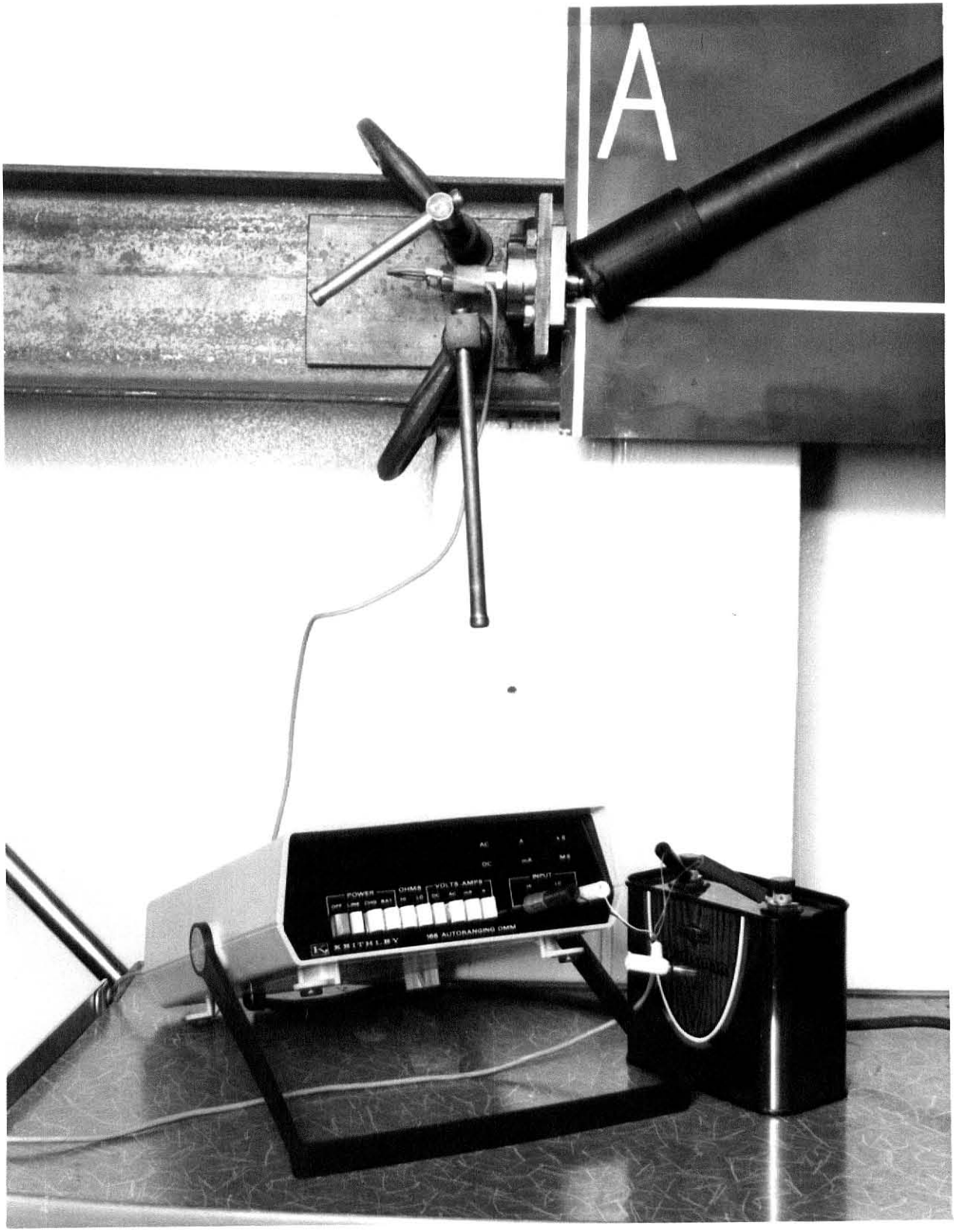

Figure 8. Experimental buckling load test apparatus

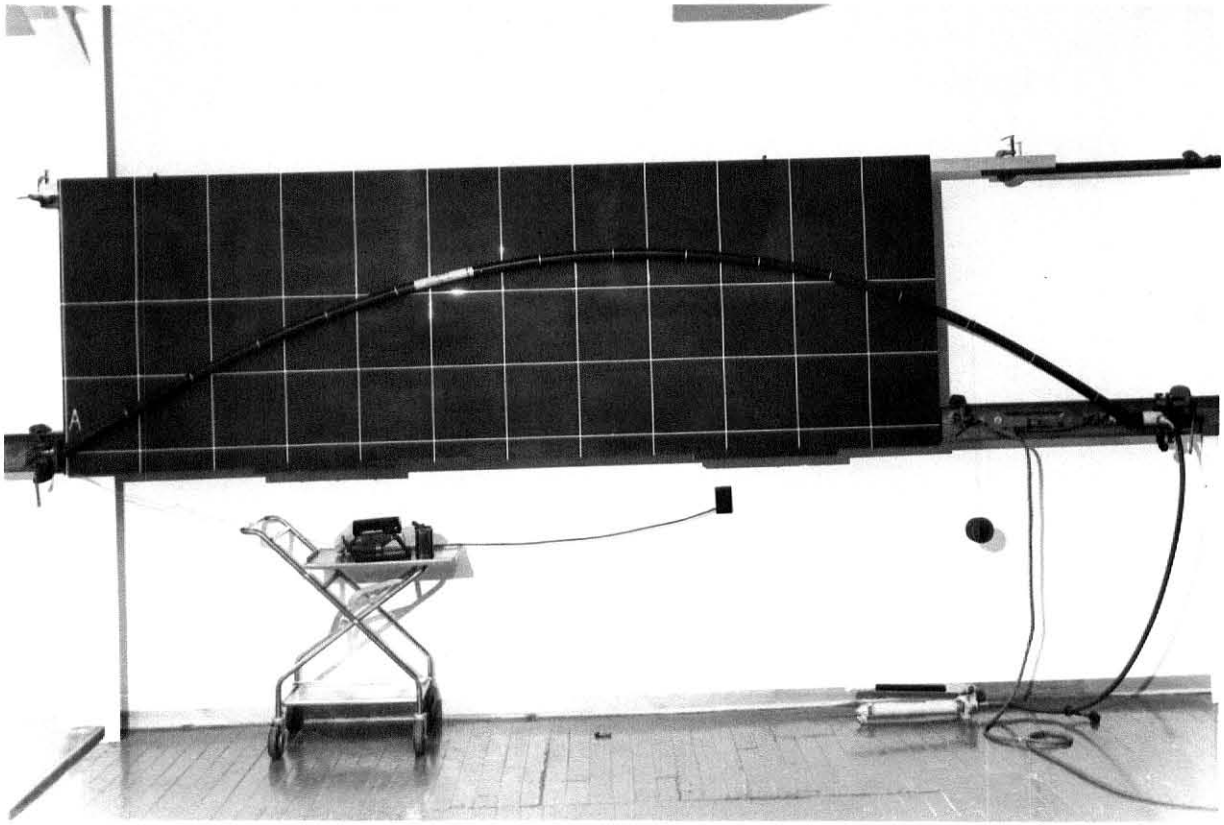

Figure 9. Experimental side load application by weights

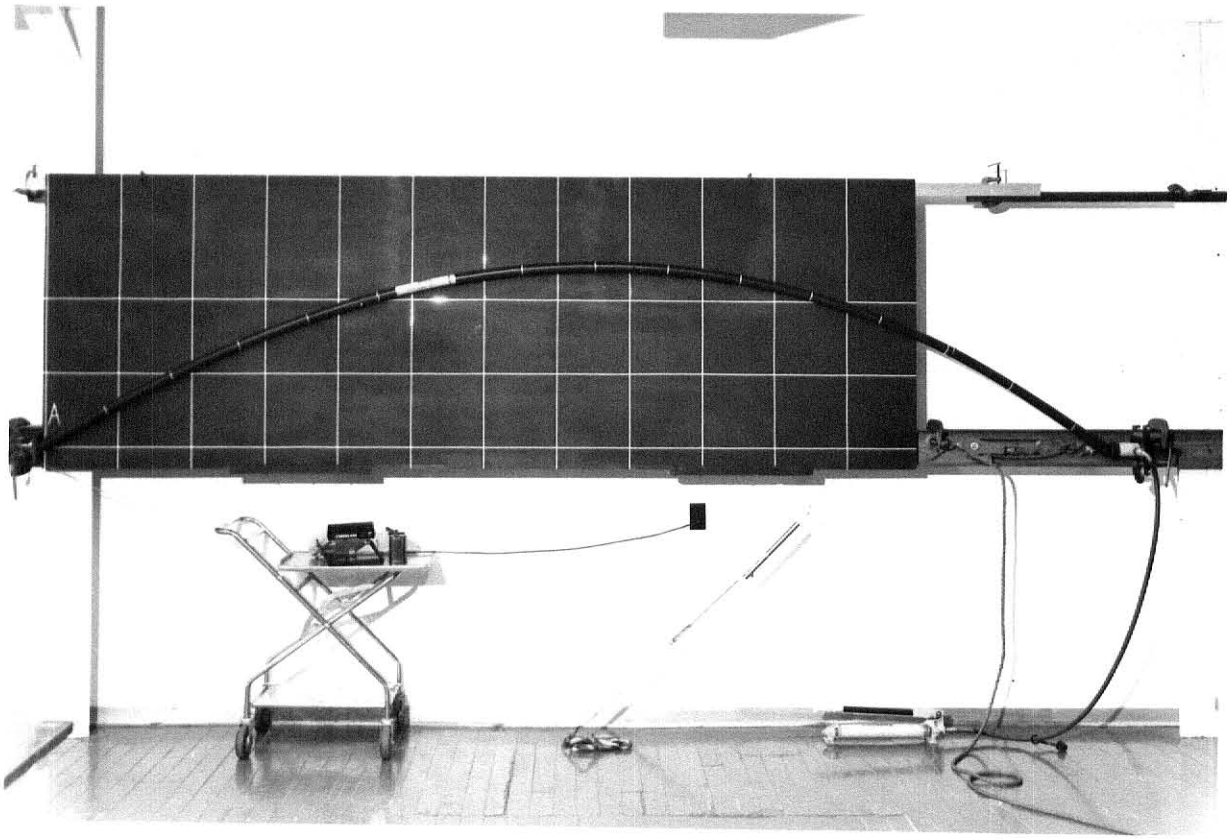

Figure 10. Experimental side load application by spring scales

$$P = 3290(V - V_{tare}) \tag{8}$$

where V is the voltage at the specified loading and V_{tare} is the voltage before the pole was introduced into the apparatus. Equation 8 was obtained by calibrating the load cell using a 50 lb standard weight.

PRESENTATION OF RESULTS

The output of the computer program was a listing, showing the configuration of the neutral axis of the pole for a specified loading (Table 2).

A comparison of experimental and numerical results is shown in Figure 11. The profile of the pole is shown in which the maximum y deflections δ for both numerical and experimental results are the same. As will be the practice in this thesis, the experimental results are shown surrounded by symbols, while a curve is plotted through the computer generated results.

The next comparison is a plot obtained by relating δ to the buckling force.

Figure 12 shows the results for pure buckling, the experimental results are surrounded by squares and the numerical results are adjacent to the experimental results. Also shown in Figure 12, either surrounded or adjacent to the circles, are the results for a 5 lb distributed load and a 5 lb point load ($\phi = 270°$). Simularly, the results are shown in Figure 13 for a 5 lb distributed load and a 10 lb point load ($\phi = 225°$). For comparison the numerical results for pure buckling are repeated in Figure 13.

These results show a comparison over the limited range of the experimental apparatus. The numerical technique was used to generate results over a broader range of loadings and deflections. Figure 14 shows a plot of maximum y deflection for various buckling loads. Curve A is for the elastica with no side loads. Curves B and C are the results for a concentrated side load F of -30 lbs and +30 lbs, respectively at an

Table 2. Numerical beam column configuration.

STANDARD POLE III
EI FROM GRAPH
LENGTH=15 FEET 7 INCH
WEIGHT= 5.00 LBS.
EPSI= 0.0100
DELT= 0.0001
F= -10.00 LBS.
PHI= 45.000 DEGREES
SF= 157.00 IN.
XF= 11.90 FEET
YF= 20.13 IN.
P= 185.00 LBS.

STIFFNESS DISTRIBUTION

450000.00 450000.00 457000.00 470000.00 500000.00 545000.00 585000.00 630000.00
665000.00 673000.00 670000.00 665000.00 665000.00 669000.00 669000.00 658000.00
650000.00 645000.00 632000.00 613000.00 577000.00 535000.00 488000.00 442000.00
397000.00 359000.00 340000.00 330000.00 325000.00 320000.00 320000.00 320000.00

S	Y	THETA	X	Y(4)
0.00000	0.00000	0.67999	0.00000	0.00000
6.23333	3.91152	0.67511	0.40444	0.40417
12.46666	7.77579	0.66067	0.81202	1.61985
18.69998	11.54648	0.63730	1.22563	3.65627
24.93329	15.18026	0.60641	1.64765	6.52799
31.16660	18.64093	0.57013	2.07964	10.25354
37.39990	21.90044	0.52990	2.52237	14.85372
43.63321	24.93498	0.48669	2.97605	20.35030
49.86652	27.72490	0.44113	3.44051	26.76505
56.09982	30.25014	0.39259	3.91535	34.11917
62.33313	32.48509	0.34028	4.40019	42.43306
68.56644	34.40146	0.28422	4.89441	51.72614
74.79974	35.97263	0.22505	5.39700	62.01620
81.03305	37.17751	0.16380	5.90656	73.31871
87.26636	38.00116	0.10109	6.42136	85.64587
93.49966	38.43166	0.03689	6.93947	99.00630
99.73297	38.45801	-0.02854	7.45881	113.40450
105.96620	38.07553	-0.09422	7.97718	128.84080
112.19950	37.28639	-0.15967	8.49235	145.31100
118.43280	36.09526	-0.22489	9.00213	162.80650
124.66610	34.50775	-0.29036	9.50435	181.31440
130.89950	32.52692	-0.35667	9.99676	200.81730
137.13280	30.15657	-0.42378	10.47708	221.29330
143.36610	27.40376	-0.49119	10.94301	242.71600
149.59940	24.28221	-0.55778	11.39252	265.05410
155.83270	20.81464	-0.62158	11.82406	288.27310
162.06600	17.03789	-0.67899	12.23721	312.33690
168.29930	13.00497	-0.72656	12.63322	337.20940
174.53260	8.77777	-0.76187	13.01493	362.85910
180.76590	4.42122	-0.78359	13.38642	389.26120
186.99920	0.00002	-0.79093	13.75258	416.40010

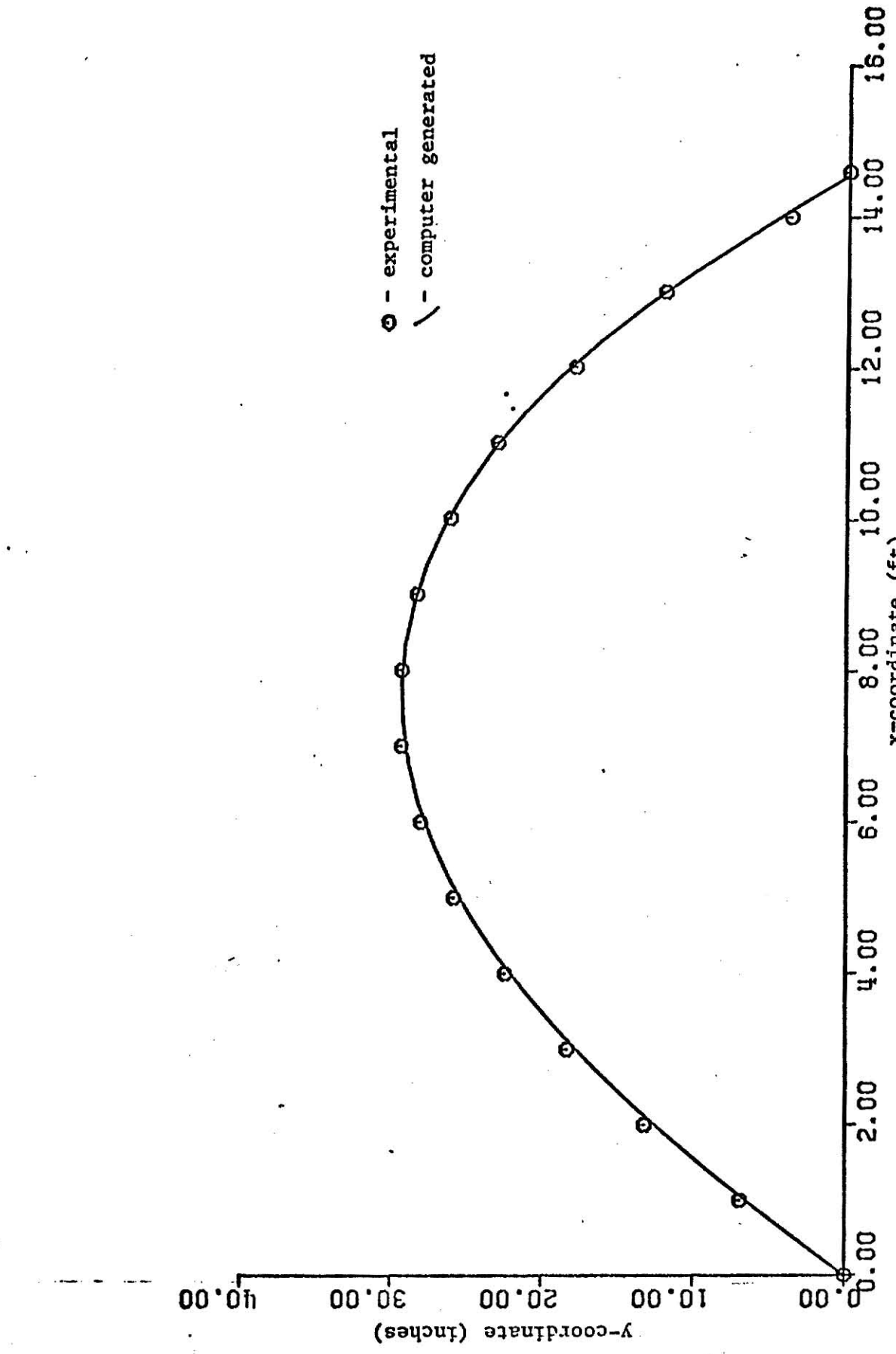

Figure 11. Numerical and Experimental Pole Profiles.

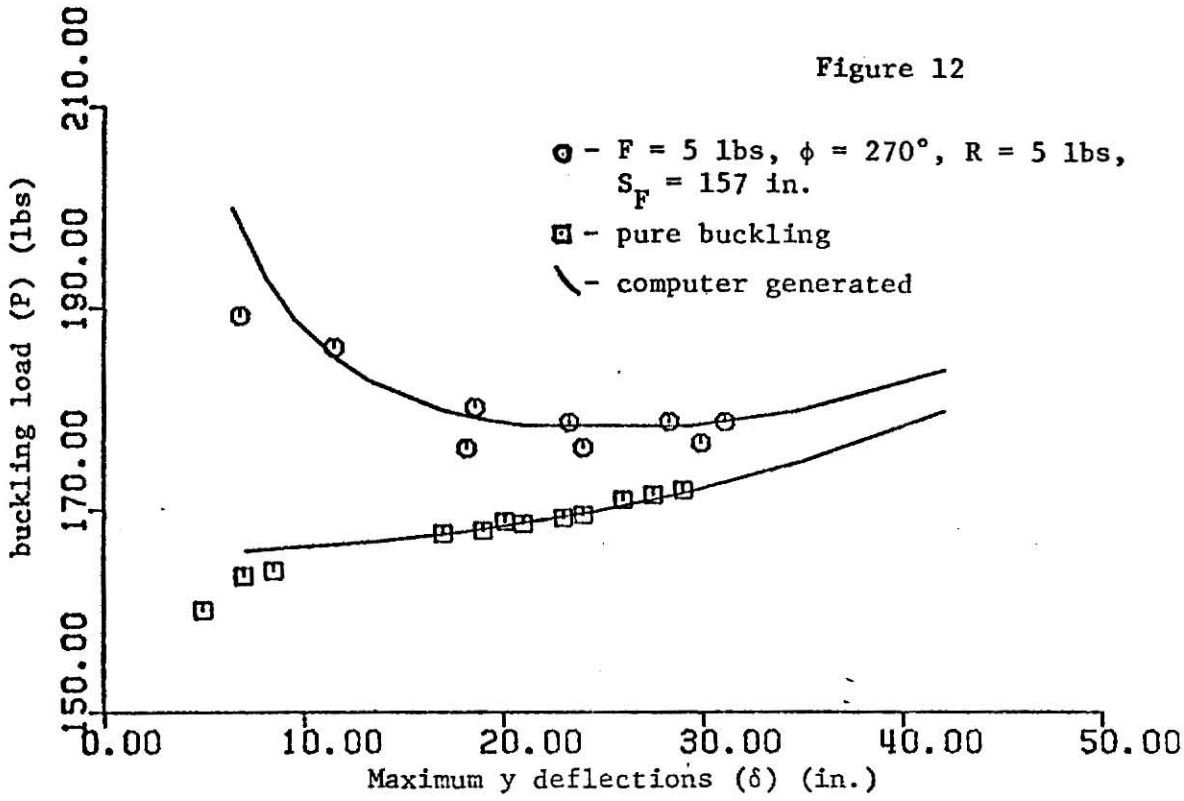

Figure 12

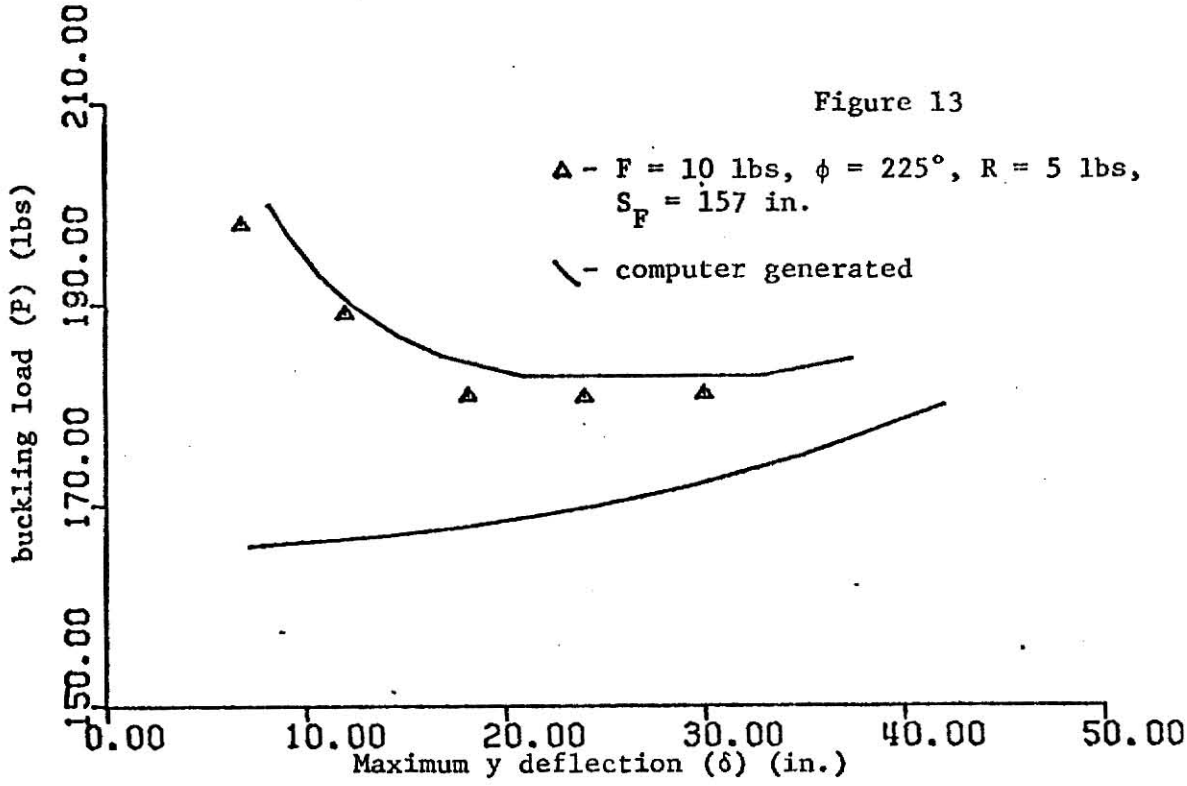

Figure 13

Figures 12 and 13. Experimental and numerical force deflection relationships.

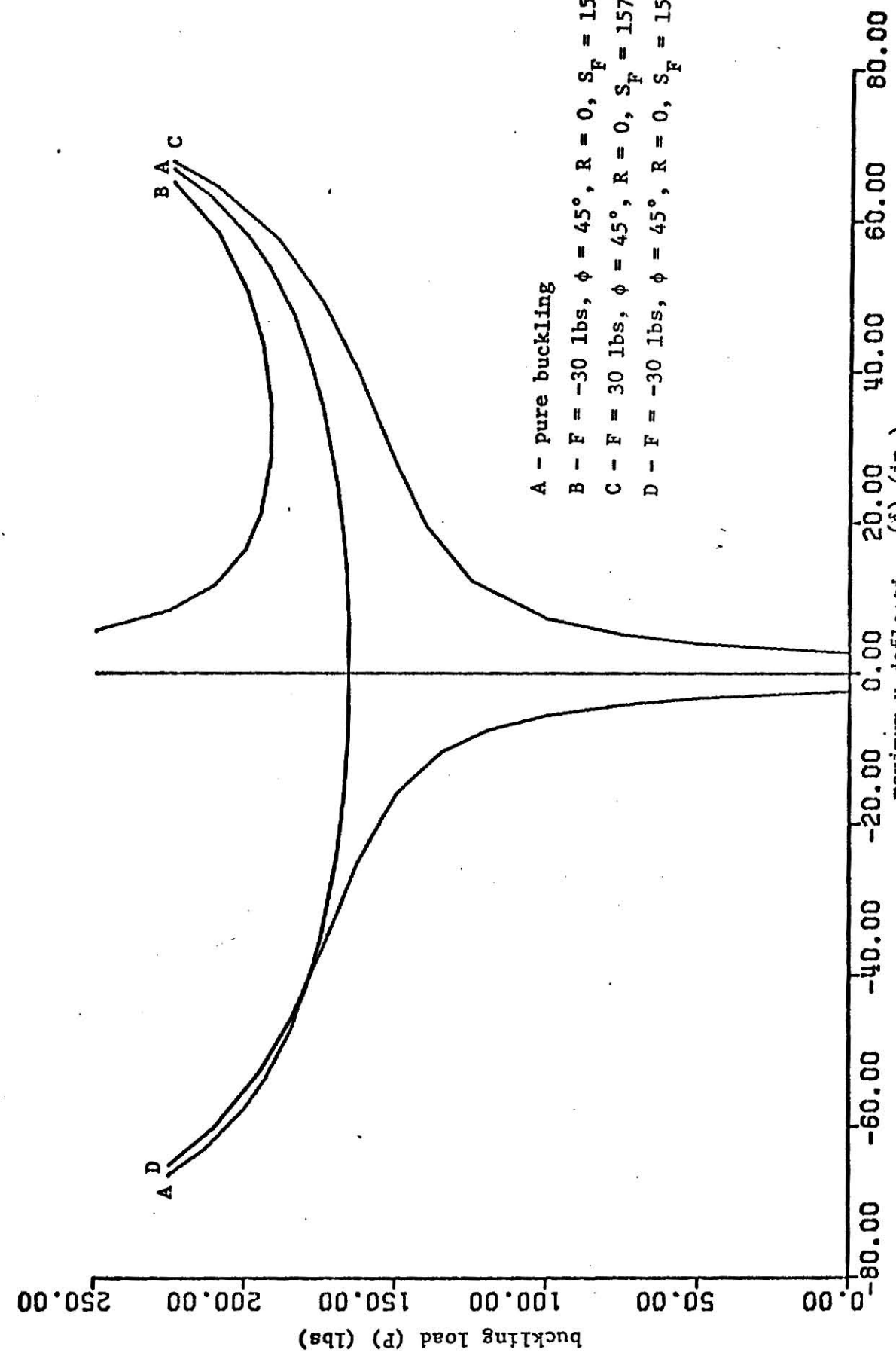

Figure 14. Numerical force deflection relationship.

angle ϕ of 45 degrees. These curves bound curve A as expected. Curve D represents the same loading as curve B but the deflection was negative (If the deflection were positive, the loading would have been: F = 30 lbs, ϕ = 135°). Note that curve D crosses curve A. This is due to the direction of the side load. When the x component of the side load is in the same direction as the load at s=L, this load must be less than P. Therefore there is in effect a shortening of the length that the buckling force acts over, which results in a stiffer system.

Next observe Figure 15. The side load is perpendicular to the unbent axis and consequently curves C and D are symmetric with respect to the ordinate.

Note the portion of curves B which are left of the relative minimum values. Although experimental data was acquired in this region, these are considered to be unstable equilibrium points. In the limit, as the side load approaches zero, this part of a curve B becomes the vertical axis which is a known unstable equilibrium position for a pure buckling problem. An envelope through the critical buckling point, points 3, and 6, bound the unstable region for this type of loading.

Consider two examples of predicted behavior near this envelope.

1. The loading is such that point 1 is indicated. The side load is decreased and reversed while the buckling force is held constant. One will observe a smooth transition from point 1 across curves C, through curve A, and across to the instability envelope. At that point snap through should occur and a jump from point 3 to point 4 should occur.

The transition should then continue smoothly from point 4 to point 5. This phenomenon is also shown on Figure 16 which is a plot of maximum y

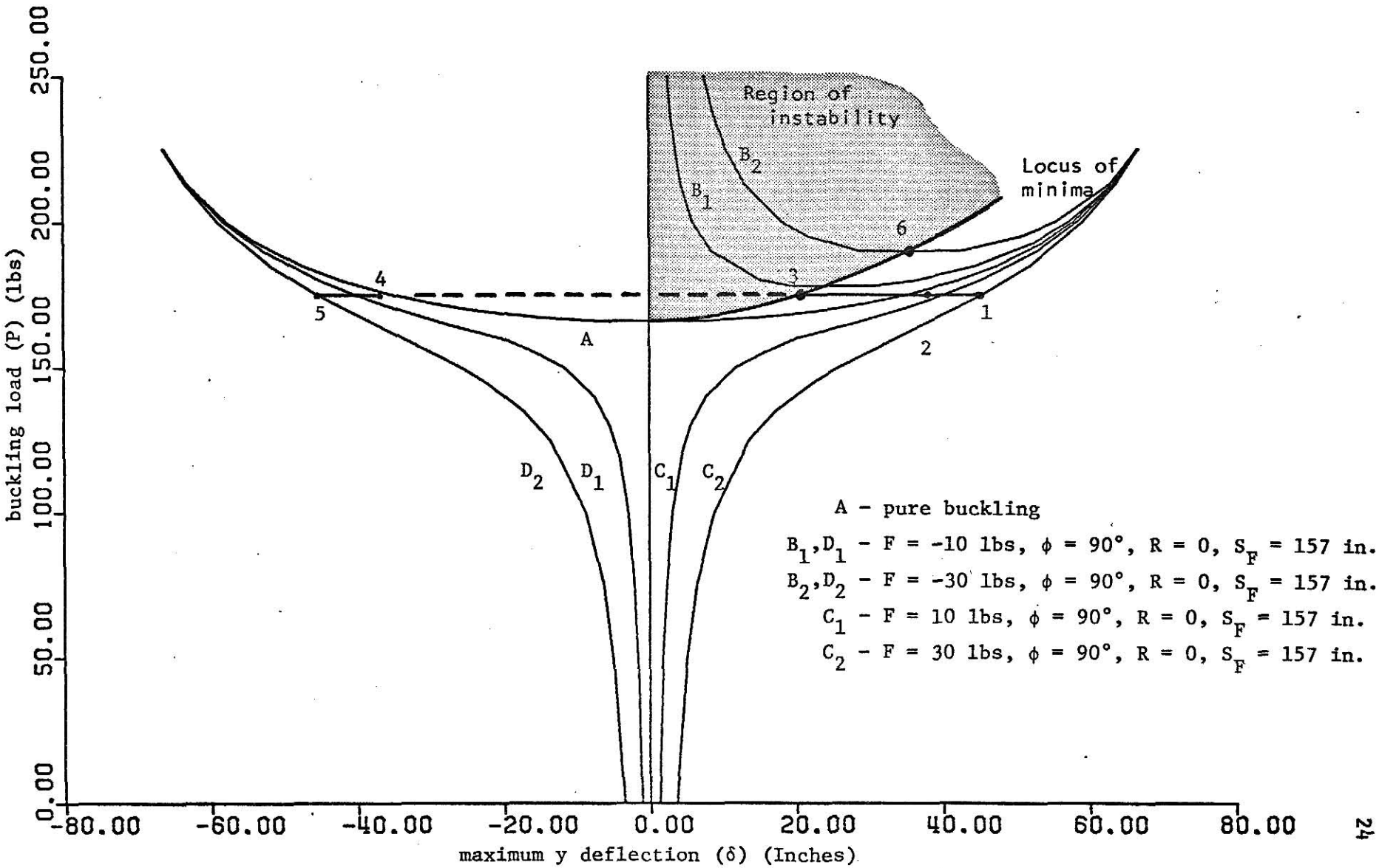

Figure 15. Numerical force deflection relationship.

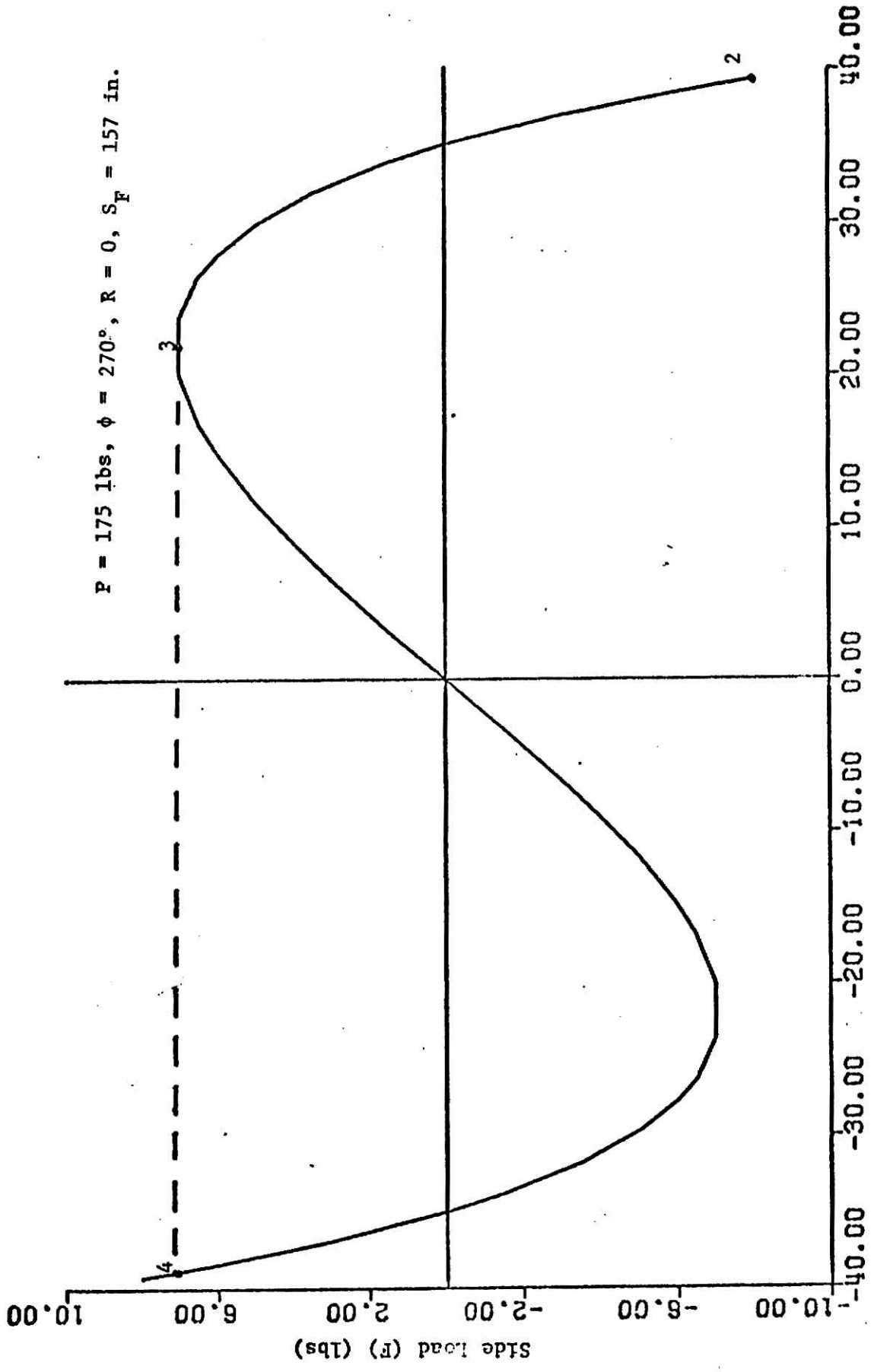

Figure 16. Numerical force deflection relationship.

deflection for various magnitudes of side load. Points 2, 3, and 4 represent the same loadings and deflections as described above.

2. The loading is such that point 6 is indicated. If the side load is held constant and the buckling load is increased, the preferred direction is that of larger deflection, and not into the unstable region.

Figure 17 shows the relationship between the maximum y deflection and x(L). The plot shown is for no side load but for all practical purposes the relation is the same for all reasonable loading conditions.

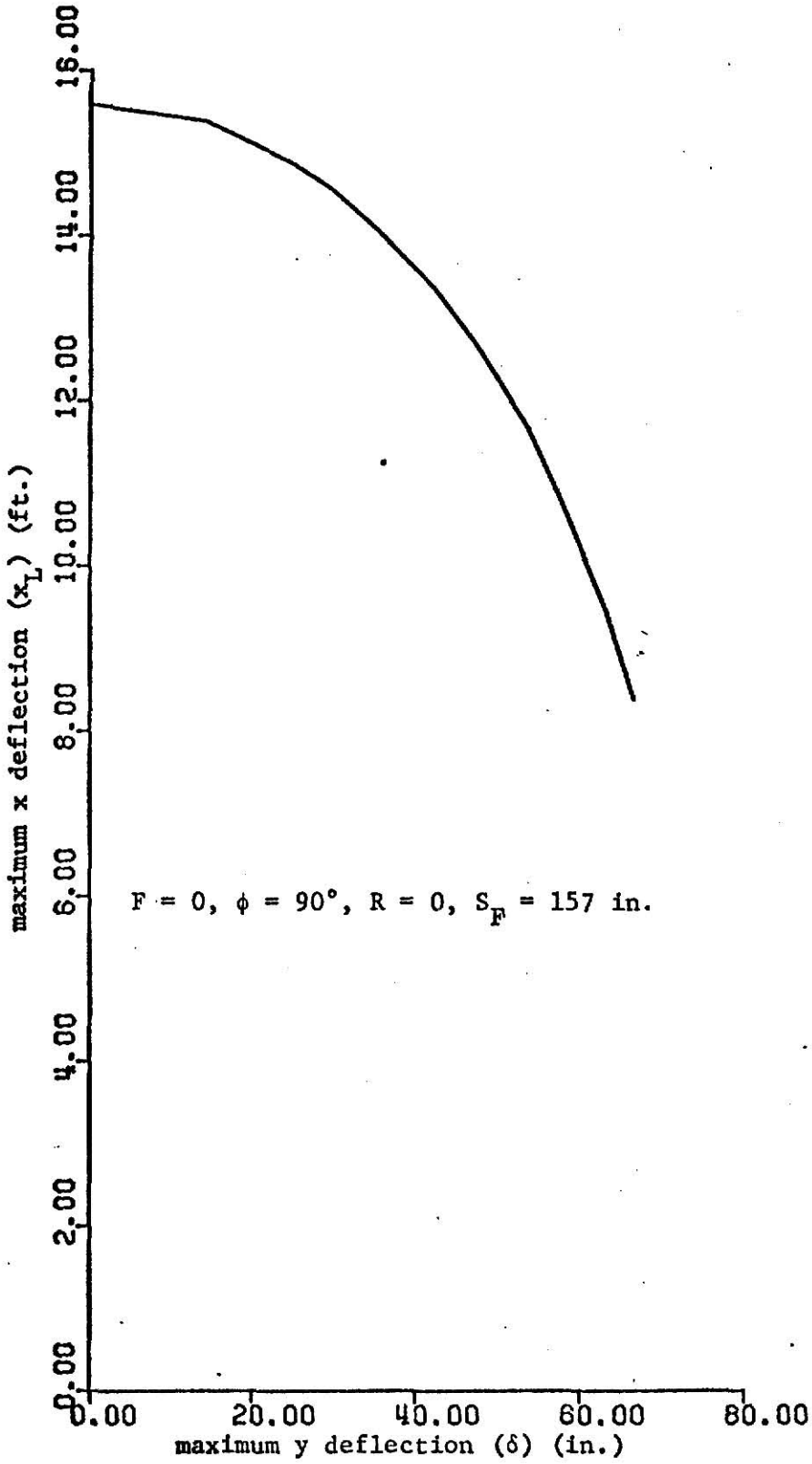

Figure 17. Numerical comparison of x and y deflections for various buckling loads.

DISCUSSION AND CONCLUSIONS

The numerical shooting method consisting of the fourth order Runge-Kutta-Gill numerical integrating technique, Lagrangian extrapolations, and a modified Newton's method appears to be an efficient and accurate method for solving this problem. The agreement between experimental and numerical data appears to be very good. The percent difference between any two comparable points is small.

One should remember that the numerical data was also based on experimental measurements. This is a place in this scheme where error may easily be introduced into the solution. A method which would determine this stiffness function easily and accurately would add to the desirability of this scheme. Possibly the coupling of a finite difference technique with linear bending of a beam would solve the problems encountered in the technique that was used.

The rate of convergence of the numerical scheme is extremely dependent on the initial guess of $\theta(0)$. Obviously, when closer to the true value of $\theta(0)$, fewer iterations are necessary. Also, in the range where two solutions exist, the solution acquired depends on the value of $\theta(0)$. If for a particular loading, $\theta(0)$ is assumed small, the solution will be the one with least y deflection. Guessing $\theta(0)$ greater than about 0.7 radians usually assures convergence to the solution with greatest y deflection, which is the stable solution. If one is seeking a solution for a buckling load that lies below the relative minimum of the curves B, Figures 14 and 15, the solution lies on a curve D and the y deflections and $\theta(0)$ are negative. If a positive $\theta(0)$ is assumed, convergence may or may not occur.

Every attempt has been made to reduce the effect of the users guess on obtaining the desired solution.

Yet, a certain level of understanding of the physical response of the system to different loads is necessary to ensure that the solution acquired is the desired solution, and, to ensure that convergence to any solution will occur.

BIBLIOGRAPHY

1. Brush, D. O. and Almroth, B. O., Buckling of Bars, Plates, and Shells, McGraw-Hill, New York, 1975.

2. Chajes, A., Principles of Structural Stability, Prentice-Hall, New Jersey, 1974.

3. Conte, S. D., Elementary Numerical Analysis, McGraw-Hill, New York, 1965, pp. 268-271.

4. Langhaar, H. L., Energy Methods in Applied Mechanics, Wiley, New York, 1962, pp. 203-206.

5. McCormick, J. M. and Salvadori, M. G., Numerical Methods in FORTRAN, Prentice-Hall, New Jersey, 1964.

6. Ralston, A. and Wilf, H. S., editors, Mathematical Methods for Digital Computers, Vol. 1, Wiley, New York, 1960, pp. 114-116.

7. Schmidt, R. and DaDeppo, D. A., "Variational Formulation of Nonlinear Equations for Straight Elastic Beams," The Journal of the Industrial Mathematics Society, Volume 23, Part 2, 1974, pp. 117-136.

8. Timoshenko, S. P. and Young, D. H., Elements of Strength of Materials, 4th ed., Van Nostrand, New Jersey, 1962, pp. 111-114.

9. Timoshenko, S. P., History of Strength of Materials, McGraw-Hill, New York, 1953, pp. 28-36.

10. Timoshenko, S. P., Strength of Materials, 3rd ed., Van Nostrand, New York, 1960.

11. Walker, H. S. and Kirmser, P. G., A Computer Analysis of the Pin Ended Elastica of Arbitrary Stiffness Distribution, Institute for Computational Research in Engineering, Report Number 74.01, Seaton Hall, Kansas State University, Manhattan, Kansas, 1974.

APPENDIX A

DERIVATION OF MODIFIED NEWTONS METHOD

Expressing as an initial value problem

$$\bar{y}(0) = \begin{Bmatrix} 0 \\ \theta_{(0)} \\ 0 \\ 0 \end{Bmatrix} = \begin{Bmatrix} 0 \\ y_{2(0)} \\ 0 \\ 0 \end{Bmatrix}$$

Also the value of the reaction at the s=0 end (R_2) is unknown.

The conditions that must be satisfied at the s=L end are

$$y(L) = 0$$

$$M(L) = 0$$

Therefore one may consider a mapping of y(L) on the $y_{2(0)}$ & R_2 planes and a mapping of M(L) on the $y_{2(0)}$ & R_2 planes

$$y_{1L} = y_{1L}(y_2(0), R_2)$$

$$M_L = M_L(y_2(0), R_2)$$

By use of the Taylor series of two independent variables one can generate a scheme to select the next iterates.

For simplicity, let

$$y = y(\theta, R_2)$$

$$M = M(\theta, R_2)$$

and let θ1, θ2, R1, R2 be assumed values of θ and R_2 then

Y1 = y(θ1,R1)	M1 = M(θ1,R1)
Y2 = y(θ2,R1)	M2 = M(θ2,R1)
Y3 = y(θ1,R2)	M3 = M(θ1,R2)

By Taylor series

$$y = Y1 + \delta\theta \frac{\partial Y1}{\partial \theta} + \delta R_2 \frac{\partial Y1}{\partial R_2}$$

$$M = M1 + \delta\theta \frac{\partial M1}{\partial \theta} + \delta R_2 \frac{\partial M1}{\partial R_2}$$

one can approximate the partial derivatives by

$$\frac{\partial Y1}{\partial \theta} = \frac{Y2 - Y1}{\theta 2 - \theta 1} \qquad \frac{\partial M1}{\partial \theta} = \frac{M2 - M1}{\theta 2 - \theta 1}$$

$$\frac{\partial Y1}{\partial R_2} = \frac{Y3 - Y1}{R2 - R1} \qquad \frac{\partial M1}{\partial R_2} = \frac{M3 - M1}{R2 - R1}$$

the desired values are y=0, M=0

$$Y1 + \delta\theta \left[\frac{Y2 - Y1}{\theta 2 - \theta 1}\right] + \delta R_2 \left[\frac{Y3 - Y1}{R2 - R1}\right] = 0$$

$$M1 + \delta\theta \left[\frac{M2 - M1}{\theta 2 - \theta 1}\right] + \delta R_2 \left[\frac{M3 - M1}{R2 - R1}\right] = 0$$

$$\delta\theta = \left\{-\delta R_2 \left[\frac{Y3 - Y1}{R2 - R1}\right] - Y1\right\} / \left[\frac{Y2 - Y1}{\theta 2 - \theta 1}\right]$$

$$0 = M1 + \left\{-\delta R_2 \left[\frac{Y3 - Y1}{R2 - R1}\right] - Y1\right\} \left[\frac{\theta 2 - \theta 1}{Y2 - Y1}\right]\left[\frac{M2 - M1}{\theta 2 - \theta 1}\right] + \delta R_2 \left[\frac{M3 - M1}{R2 - R1}\right]$$

$$\delta R = \frac{M1 - Y1\left[\frac{M2 - M1}{Y2 - Y1}\right]}{\left[\frac{Y3 - Y1}{Y2 - Y1}\right]\left[\frac{M2 - M1}{R2 - R1}\right] - \frac{M3 - M1}{R2 - R1}}$$

$$R_2 = R1 + \delta R_2$$

$$R_2 = R1 + \left\{M1 - Y1\left[\frac{M2 - M1}{Y2 - Y1}\right]\right\} [R2 - R1] / \left\{\left[\frac{Y3 - Y1}{Y2 - Y1}\right][M2 - M1] - [M3 - M1]\right\}$$

$$R_2 = R1 + \left\{[M1(Y2 - Y1) - Y1(M2 - M1)](R2 - R1)\right\} / (Y3 - Y1)(M2 - M1) \cdot$$

$$- (M3 - M1)(Y2 - Y1)\Big\}$$

Similarly

$$\theta = \theta 1 + \left\{[Y1(M3 - M1) - M1[Y3 - Y1)](\theta 2 - \theta 1]\right\} / \left\{(M2 - M1)(Y3 - Y1) - (Y2 - Y1)(M3 - M1)\right\}$$

When the sideloads are zero this may be reduced to

$$y = y(\theta)$$

$$Y1 = y(\theta 1)$$

$$Y2 = y(\theta 2)$$

By Taylor series

$$y = Y1 + \delta\theta \frac{\partial Y_1}{\partial \theta}$$

Approximate $\frac{\partial Y_1}{\partial \theta}$ by $\frac{Y2 - Y1}{\theta 2 - \theta 1}$

$$y = Y1 + \delta\theta \left(\frac{Y2 - Y1}{\theta 2 - \theta 1}\right)$$

for y = 0

$$Y1 + \delta\theta \left(\frac{Y2 - Y1}{\theta 2 - \theta 1}\right) = 0$$

$$\delta\theta = -Y1 \left(\frac{\theta 2 - \theta 1}{Y2 - Y1}\right)$$

$$\theta = \theta 1 + \delta\theta$$

$$\theta = \theta 1 - Y1 \left(\frac{\theta 2 - \theta 1}{Y2 - Y1}\right)$$

APPENDIX B

Vector Formulation of the Differential Equations

For use in the computer program it is necessary to cast the problem in vector notation.

The independent variables were selected to be $\bar{Y}$.

$$\bar{Y} = \begin{Bmatrix} Y_1 \\ Y_2 \\ Y_3 \\ Y_4 \end{Bmatrix} = \begin{Bmatrix} y \\ \theta \\ x \\ M_w \end{Bmatrix}$$

$$X = s$$

$$\bar{Y}' = \begin{Bmatrix} Y_1' \\ Y_2' \\ Y_3' \\ Y_4' \end{Bmatrix} = \begin{Bmatrix} \sin Y_2 \\ M/EI \\ \cos Y_2 \\ w\ Y_3 \end{Bmatrix} = \begin{Bmatrix} \sin \theta \\ M/EI \\ \cos \theta \\ wx \end{Bmatrix}$$

for $$0 \leq X \leq X_F$$

$$M = -PY_1 + (R_2 - wX)Y_3 + Y_4$$

for $$X_F \leq X \leq L$$

$$M = -(P + F\cos\phi)Y_1 + (R_2 - wX + F\sin\phi)Y_3 + Y_4 + Fy_F\cos\phi - Fx_F\sin\phi$$

and since the last two terms remain constant

$$M = -(P + F\cos\phi)Y_1 + (R_2 - wX + F\sin\phi)Y_3 + Y_4 + M_F$$

APPENDIX C

Listing of Computer Program

ILLEGIBLE DOCUMENT

THE FOLLOWING DOCUMENT(S) IS OF POOR LEGIBILITY IN THE ORIGINAL

THIS IS THE BEST COPY AVAILABLE

```
$JOB          PDC,TIME=(0,10),NOLIST
      DIMENSION Y(4),DY(4),O(4),BETA(32)
      DIMENSION Y2(31),Y4(31),Y1S(3),Y2S(2),R2S(2),DY2S(3)
      COMMON P,W,R2,II,Y1(31),Y3(31),YF,XF,FY,FX,XFF,FMOM,SF,XX(31)
  600 FORMAT(8F10.2)
  601 FORMAT(////,11X,'S',14X,'Y',12X,'THETA',12X,'X',12X,'Y(4)')
  602 FORMAT(1H1)
  603 FORMAT(4F10.4)
  604 FORMAT(F10.4,20X,F10.4)
  200 FORMAT(5F15.5)
   10 FORMAT(' ','STANDARD POLE III   ',/,' EI FROM GRAPH',/,
     C' LENGTH=15 FEET 7 INCH',/,' WEIGHT=',F6.2,' LBS.',/,
     C' EPSI=',F10.4,/,' DELT=',F10.4)
   20 FORMAT(' F=',F11.2,' LBS.',/,' PHI=',F10.3,' DEGREES',
     C/,' SF=',F10.2,' IN.',
     C/,' XF=',F10.2,' FEET',/,' YF=',F10.2,' IN. ',/,
     C' P=',F11.2,' LBS.',///,' STIFFNESS DISTRIBUTION',/)
      NBETA=32
C     THE POLE STIFFNESS (BETA) IS READ FOR AT LEAST NSTEP+1
C     EVENLY DISTRIBUTED POINTS, STARTING AT S=0 AND SEPARATED
C     BY H=L/NSTEP
      READ(5,600) (BETA(I),I=1,NBETA)
C     THE LOCATION (SF), DIRECTION (PHI), AND MAGNITUDE (F)
C     OF THE SIDE LOAD IS ASSIGNED
      SF=157.0
      PHI=45.
      F=-10.
C     F IS RESOLVED INTO COMPONENTS IN THE X AND Y DIRECTION
      PHIRAD=PHI*3.1415926/180.
      FX=F*COS(PHIRAD)
      FY=F*SIN(PHIRAD)
C     DELT & EPSI ARE THE REQUIRED ACCURACIES OF Y(L) & M(L)
      DELT=0.0001
      EPSI=100.0*DELT
C     R IS THE TOTAL DISTRIBUTED WEIGHT OF THE POLE
      R=5.0
C     P IS THE BUCKLING LOAD AT THE POLE BOX END
      P=185.0
      KSTOP=0
      NEQ=4
      NSTEP=30
      H=(15.0*12.0+7.0)/NSTEP
      R1=R
      W=R/(H*NSTEP)
      WRITE(6,602)
C     Y2S IS THE INITIAL GUESS OF THETA
C     R2S IS THE INITIAL GUESS OF R2
C     Y1S IS THE RESULTANT Y DEFLECTION AT S=L
C     DY2S IS THE RESIDUAL MOMENT AT S=L
C     IF     Y2S(1) & R2S(1)     THEN     Y1S(1) & DY2S(1)
C     IF     Y2S(2) & R2S(1)     THEN     Y1S(2) & DY2S(2)
C     IF     Y2S(1) & R2S(2)     THEN     Y1S(3) & DY2S(3)
      Y2S(1)=0.8
      Y2S(1)=0.2
      Y2S(1)=1.0
      Y2S(2)=1.1*Y2S(1)
      R2S(1)=R/2.-(1.-SF/H/NSTEP)*FY
      R2S(2)=1.1*R2S(1)
      K=1
C     THE FLAG K=4 CAUSES THE SIMPLIFIED NEWTONS METHOD TO BE
```

```
C     USED FOR THE CASE OF NO SIDE LOAD
      IF(R.EQ.0.0.AND.FY.EQ.0.0) K=4
      IF(R2S(2).EQ.R2S(1)) R2S(2)=R2S(1)+0.1
      K1=1
      K2=1
C     * * * * * * * * * * * * * * * * * * * * * * * * * * * * * * * *
C     INTEGRATION BEGINS
  500 Y(1)=0.0
      Y(2)=Y2S(K1)
      Y(3)=0.0
      Y(4)=0.0
      R2=R2S(K2)
      X=0.0
      Q(1)=0.0
      Q(2)=0.0
      Q(3)=0.0
      Q(4)=0.0
      XX(1)=X
      Y1(1)=Y(1)
      Y2(1)=Y(2)
      Y3(1)=Y(3)
      Y4(1)=Y(4)
      DO 100 I=1,NSTEP
      IBETA=1
      II=I+1
      CALL RKG(NEQ,H,X,Y,DY,Q,BETA,NBETA,IBETA)
      XX(II)=X
      Y1(II)=Y(1)
      Y2(II)=Y(2)
      Y3(II)=Y(3)/12.0
      Y4(II)=Y(4)
  100 CONTINUE
      DY2=(FMOM-(P+FX)*Y(1)+(R2+FY-W*X)*Y(3)+Y(4))
      IF(ABS(Y(1)).LT.DELT.AND.ABS(DY2).LT.EPSI) GO TO 700
C     KSTOP ELIMINATES THE POSSIBILITY OF AN INFINATE LOOP
C     WHEN CONVERGENCE DOES NOT OCCUR
      KSTOP=KSTOP+1
      IF(KSTOP.GT.25) GO TO 999
C     * * * * * * * * * * * * * * * * * * * * * * * * * * * * * * * *
C     INFORMATION IS SAVED AND THE NEXT ITERATES DETERMINED
      GO TO (801,801,802,803,804),K
  801 Y1S(K)=Y(1)
      DY2S(K)=DY2
      K1=1
      IF(K.EQ.2) K2=2
      K=K+1
      IF(K.EQ.2) K1=2
      GO TO 500
  802 Y1S(K)=Y(1)
      DY2S(K)=DY2
      WRITE(6,603) (Y1S(I),Y2S(I),R2S(I),DY2S(I),I=1,2)
      WRITE(6,604) Y1S(3),DY2S(3)
      Y2TEMP=FUTURE(Y2S,Y1S,DY2S,3,2)
      R2TEMP=FUTURE(R2S,DY2S,Y1S,2,3)
      R2S(2)=R2S(1)
      R2S(1)=R2TEMP
      Y2S(2)=Y2S(1)
      Y2S(1)=Y2TEMP
      K=1
      K2=1
```

```
      GO TO 500
  803 Y1S(K-3)=Y(1)
      WRITE(6,604) Y1S(1),Y2S(1)
      K1=2
      K=K+1
      GO TO 500
  804 Y1S(K-3)=Y(1)
      WRITE(6,604) Y1S(2),Y2S(2)
      Y2TEMP=Y2S(1)-Y1S(1)*(Y2S(2)-Y2S(1))/(Y1S(2)-Y1S(1))
      Y2S(1)=Y2S(2)
      Y1S(1)=Y1S(2)
      Y2S(2)=Y2TEMP
      GO TO 500
  700 WRITE(6,603) Y(1),Y2S(K1),R2S(K2),DY2
      WRITE(6,602)
      WRITE(6,10) R1,EPSI,DELT
      WRITE(6,20) F,PHI,SF,XFF,YF,P
      WRITE(6,600) (BETA(I),I=1,NBETA)
      WRITE(6,601)
      NSTEP1=NSTEP+1
      WRITE(6,200) (XX(I),Y1(I),Y2(I),Y3(I),Y4(I),I=1,NSTEP1)
      WRITE(6,602)
  999 STOP
      END
      SUBROUTINE PKG(NEQ,H,X,Y,DY,Q,BETA,NBETA,IBETA)
C     * * * * * * * * * * * * * * * * * * * * * * * * * * * * * * * * *
C     THE INDEPENDENT VARIABLE X IS INCREMENTED IN THIS PROGRAM
C     Y(I) AND DY(I) ARE THE DEPENDENT VARIABLE AND ITS DERIVATIVE
C     ALL THE Q(I) MUST BE INITIALLY SET TO ZERO IN THE MAIN PROGRAM
C     NEQ = NUMBER OF FIRST ORDER EQUATIONS
C     H = INTERVAL SIZE
C     A SUBROUTINE DERIV(NEQ,X,Y,DY,B) MUST BE PROVIDED
C     * * * * * * * * * * * * * * * * * * * * * * * * * * * * * * * * *
      DIMENSION BETA(NBETA)
      DIMENSION  A(2)
      DIMENSION Y(NEQ),DY(NEQ),Q(NEQ)
      A(1)=0.29289321881345475
      A(2)=1.7071067811865475
      H2=.5*H
      BB=BETA(IBETA)
      CALL DERIV(NEQ,X,Y,DY,BB)
      DO 13 I=1,NEQ
      B=H2*DY(I)-Q(I)
      Y(I)=Y(I)+B
   13 Q(I)=Q(I)+3.*B-H2*DY(I)
      X=X+H2
      BB=(BETA(IBETA)+BETA(IBETA+1))/2.0
      DO 20 J=1,2
      CALL DERIV(NEQ,X,Y,DY,BB)
      DO 20 I=1,NEQ
      B=A(J)*(H*DY(I)-Q(I))
      Y(I)=Y(I)+B
   20 Q(I)=Q(I)+3.*B-A(J)*H*DY(I)
      X=X+H2
      BB=BETA(IBETA+1)
      CALL DERIV(NEQ,X,Y,DY,BB)
      DO 26 I=1,NEQ
      B=0.16666666666666666*(H*DY(I)-2.*Q(I))
      Y(I)=Y(I)+B
   26 Q(I)=Q(I)+3.*B-H2*DY(I)
```

```
      RETURN
      END
      SUBROUTINE DERIV(NEQ,X,Y,DY,B)
C     * * * * * * * * * * * * * * * * * * * * * * * * * * * * * * * *
C     THE DERIVATIVES OF THE VECTOR DIFFERENTIAL EQUATION
C     ARE EVALUATED IN THIS SUBROUTINE
C     * * * * * * * * * * * * * * * * * * * * * * * * * * * * * * * *
      DIMENSION Y(NEQ),DY(NEQ)
      COMMON P,W,R2,II,Y1(31),Y3(31),YF,XF,FY,FX,XFF,FMOM,SF,XX(31)
      DY(1)=SIN(Y(2))
      DY(3)=COS(Y(2))
      DY(4)=W*Y(3)
      IF(X.LE.SF) GO TO 10
      IF(KK.EQ.1) GO TO 20
   30 DY(2)=(FMOM-(P+FX)*Y(1)+(R2+FY-W*X)*Y(3)+Y(4))/B
      RETURN
   10 DY(2)=(Y(4)-P*Y(1)+(R2-W*X)*Y(3))/B
      KK=1
      RETURN
C     LAGRANGIAN EXTRAPOLATION OF N-1 DEGREE TO FIND THE X AND Y
C     COORDINATES OF THE SIDE LOAD
   20 N=4
      CALL EXTRAP(N,II,SF,XFF,XX,Y3)
      CALL EXTRAP(N,II,SF,YF,XX,Y1)
      XF=XFF*12.0
      FMOM=FX*YF-FY*XF
      KK=2
      GO TO 30
      END
      SUBROUTINE EXTRAP(N,II,XFF,YF,Y3,Y1)
C     * * * * * * * * * * * * * * * * * * * * * * * * * * * * * * * *
C     THIS SUBROUTINE USES LAGRANGIAN INTERPOLATION OF
C     N-1 DEGREE FOR EXTRAPOLATION TO DETERMINE XFF GIVEN
C     VALUES FOR N BACK POINTS.
C     * * * * * * * * * * * * * * * * * * * * * * * * * * * * * * * *
      DIMENSION Y3(31),Y1(31)
      YF=0.0
      PU=1.0
      DO 11 I=1,N
   11 PU=PU*(XFF-Y3(II-I))
      DO 13 J=1,N
      PL=1.0
      DO 12 I=1,N
      IF(I.EQ.J) GO TO 12
      PL=PL*(Y3(II-J)-Y3(II-I))
   12 CONTINUE
      PT=PU/PL/(XFF-Y3(II-J))
   13 YF=YF+PT*Y1(II-J)
      RETURN
      END
      FUNCTION FUTURE(R2S,DY2S,Y1S,L,M)
C     * * * * * * * * * * * * * * * * * * * * * * * * * * * * * * * *
C     THIS SUBROUTINE IS THE MODIFIED NEWTON'S METHOD THAT
C     GENERATES THE NEXT ITERATES FOR TWO FUNCTIONS OF TWO
C     INDEPENDENT VARIABLES.   FUTURE MUST BE CALLED TWICE
C     * * * * * * * * * * * * * * * * * * * * * * * * * * * * * * * *
      DIMENSION R2S(2),DY2S(3),Y1S(3)
      FUTURE=DY2S(1)+(Y1S(L)-Y1S(1))-Y1S(1)*(DY2S(L)-DY2S(1))
      FUTURE=(R2S(2)-R2S(1))*FUTURE
      DUMMY=(Y1S(M)-Y1S(1))*(DY2S(L)-DY2S(1))
```

```
      DUMMY=DUMMY-(DY2S(M)-DY2S(1))*(Y1S(L)-Y1S(1))
      FUTURE=R2S(1)+FUTURE/DUMMY
      RETURN
      END
$ENTRY
450000.0  450000.0  457000.0  470000.0  500000.0  545000.0  585000.0  630000.0
665000.0  673000.0  670000.0  665000.0  665000.0  669000.0  669000.0  658000.0
650000.0  645000.0  632000.0  613000.0  577000.0  535000.0  488000.0  442000.0
397000.0  359000.0  340000.0  330000.0  325000.0  320000.0  320000.0  320000.0
$STOP
```

VITA

MICHAEL D. CALDERWOOD

Candidate for the degree of

Master of Science

Thesis: NONLINEAR DEFLECTIONS OF A PIN ENDED SLENDER BEAM COLUMN OF ARBITRARY STIFFNESS

Major Field: Mechanical Engineering

Biographical:

Personal Data: Born at Topeka, Kansas, September 9, 1952, the son of Hollis D. and Thelma M. Calderwood

Education: Graduated from Seaman High School in Topeka, Kansas, in 1970; received the Bachelor of Science degree from Kansas State University, with a major in Mechanical Engineering, in December 1974

Professional Experience: Served as a graduate research assistant and graduate teaching assistant since January 1975 for the Mechanical Engineering Department.

NONLINEAR DEFLECTIONS OF A PIN ENDED SLENDER BEAM COLUMN OF ARBITRARY STIFFNESS

by

Michael Duane Calderwood

B.S., Kansas State University, 1974

AN ABSTRACT OF A MASTER'S THESIS

submitted in partial fulfillment of the

requirements for the degree

MASTER OF SCIENCE

Department of Mechanical Engineering

KANSAS STATE UNIVERSITY
Manhattan, Kansas

1977

ABSTRACT

Large deflections of a pin ended slender beam column of arbitrary stiffness distribution are investigated. The loadings considered are a buckling load, a uniformly distributed load, and a point load of arbitrary location, direction, and magnitude. The stiffness of the beam column is assumed to be nonuniform but continuous and to obey Hooke's law. Differential equations of a mathematical model are presented and a numerical scheme for solution of these equations is proposed. The scheme consists of the "shooting" method using numerical integration by the Runge-Kutta-Gill technique, extrapolation of the coordinates of the side load by Lagrangian interpolation, and a modified Newton's method for determining the proper initial conditions. A physical model is also presented as a commercial pole vaulting pole. Experimental configurations of the pole are compared with the mathematical model and the results appear to be very good. The mathematical model is further studied and predictions are made as to the large deflection behavior of this beam column. The "shooting" technique as presented appears to be an efficient technique to model the behavior of this nonlinear phenomina.